ORIGINAL RESEARCH

Mycogenic Synthesis of Extracellular Zinc Oxide Nanoparticles from *Xylaria acuta* and Its Nanoantibiotic Potential

Basavaraju Sumanth [ID][1],*
Thimappa Ramachandrappa Lakshmeesha[1],*
Mohammad Azam Ansari[2]
Mohammad A Alzohairy[3]
Arakere Chunchegowda Udayashankar[4]
Balagangadharaswamy Shobha[1]
Siddapura Ramachandrappa Niranjana[4]
Chowdappa Srinivas [ID][1],*
Ahmad Almatroudi [ID][3]

[1]Department of Microbiology & Biotechnology, Jnana Bharathi Campus, Bangalore University, Bangalore 560056, India; [2]Department of Epidemic Disease Research, Institute for Research and Medical Consultations (IRMC), Imam Abdulrahaman Bin Faisal University, Dammam 31441, Saudi Arabia; [3]Department of Medical Laboratories, College of Applied Medical Sciences, Qassim University, Qassim 51431, Saudi Arabia; [4]Department of Studies in Biotechnology, University of Mysore, Mysuru 570006, India

*These authors contributed equally to this work

Correspondence: Chowdappa Srinivas
Department of Microbiology & Biotechnology, Jnana Bharathi Campus, Bangalore University, Bangalore 560056, India
Tel +91 9972091611
Email srinivasbub@gmail.com

Ahmad Almatroudi
Department of Medical Laboratories, College of Applied Medical Sciences, Qassim University, Qassim 51431, Saudi Arabia
Email aamtrody@qu.edu.sa

Purpose: The study aimed to find an effective method for fungal-mediated synthesis of zinc oxide nanoparticles using endophytic fungal extracts and to evaluate the efficiency of synthesized ZnO NPs as antimicrobial and anticancerous agents.

Methods: Zinc oxide nanoparticles (ZnO NPs) were produced from zinc nitrate hexahydrate with fungal filtrate by the combustion method. The spectroscopy and microscopy techniques, such as ultraviolet-visible spectroscopy, Fourier transform infrared spectroscopy (FT-IR), powder X-ray diffraction (PXRD), scanning electron microscopy (SEM) with energy-dispersive X-ray spectroscopy (EDX), dynamic light scattering (DLS), and transmission electron microscopy (TEM) with selected area electron diffraction (SAED), were used to characterize the obtained product. Antibacterial activity on Gram-positive (*Staphylococcus aureus* and *Bacillus cereus*) and Gram-negative (*Pseudomonas aeruginosa* and *Escherichia coli*) samples was tested by broth microplate dilution technique. ZnO NPs antifungal activity was determined against plant pathogenic and regular contaminating fungi using the food-poison method. The anticancerous assay of the synthesized ZnO NPs was also investigated by cell uptake, MTT assay, and apoptosis assay.

Results: The fungal synthesized ZnO NPs were pure, mainly hexagonal in shape and size range of 34–55 nm. The biosynthesized ZnO NPs could proficiently inhibit both Gram-positive and Gram-negative bacteria. ZnO NPs synthesized from fungal extract exhibited antifungal activity in a dose-dependent manner with a high percentage of mycelial inhibition. The cell uptake analysis of ZnO NPs suggests that a significant amount of ZnO NPs (1 μg/mL) was internalized without disturbing cancer cells' morphology. As a result, the synthesized ZnO NPs showed significant anticancer activity against cancer cells at 1 μg/mL concentration.

Conclusion: This fungus-mediated synthesis of ZnO NPs is a simple, eco-friendly, and non-toxic method. Our results show that the synthesized ZnO NPs are an excellent novel antimicrobial and anticancer agent. Further studies are required to understand the mechanism of the antimicrobial, anticancerous action of ZnO NPs and their possible genotoxicity.

Keywords: endophytic fungi, zinc oxide nanoparticles, antibacterial, antifungal, anticancerous

Introduction

Zinc oxide nanoparticles (ZnO NPs) are an attractive choice since they are harmless to the human body and environment at minimum concentrations and have broad-spectrum antimicrobial activities.[1] Interactions between microorganisms and nanostructured substances are receiving increased attention due to the possibility of synthesizing efficient bio-nano materials with specific biological activities.[2,3] There is a significant turn of

events in innovative green synthesis processes that yield nanoscale biocompatible nanoparticles. These particles are utilized to test biological routes and analyze applications in the biomedical field.[4] Recent research attention to biological nanomaterials has led to the availability of a substantial amount of information.[5] To accomplish the previously stated biological nanoscience points, the reductants, solvents, and ligating agents for nanoparticle synthesis have already been examined.[6] A natural well-disposed nanoparticle combination technique does not utilize any toxic chemicals in the amalgamation procedures. Accordingly, these engineered strategies dependent on naturally occurring biomaterials provide an elective way to acquiring industrially required nanoparticles.[7,8]

The production of ZnO NPs with inorganic complex, utilizing natural obtained ligating agents produced from biological resources, is one of the push zones of attention for biological nanostructures investigation. ZnO is one of the most significant semiconducting resources due to versatile applications and exceptional properties.[9] ZnO takes a steady wurtzite arrangement containing several planes composed of tetrahedral synchronized Zn^{2+} and O^- ions, placed one after the other along the c-axis.[10] ZnO is an ecologically available material and is biocompatible, which is required, particularly for applications in the biomedical field.[11] It has been demonstrated that the green amalgamation of NPs is eco-friendly, involves minimal effort, and is less harmful when contrasted with other physical and synthetic chemical synthesis strategies. Aside from the previously mentioned properties, these ZnO NPs integrated through fungal extracts are additionally known to have useful antibacterial properties.[12]

Millingtonia hortensis L.f. is a well-branched tree that comes under the family *Bignoniaceae* and is naturally found in South and Southeast Asia. It was extensively used in ancient medicine because of its aromatic compounds and perceived antifungal, antibacterial, anticancerous, and anti-inflammatory properties. Hence, endophytic fungi present might possess similar potential secondary metabolites responsible for the above-mentioned properties.[13–15] Many endophytic fungi have been utilized to determine extracellular biomass free production of metal nanoparticles, such as *Penicillium* sp., *Aspergillus flavus*, and *Verticillium* sp.[16] Due to their metal bioaccumulation capacity and tolerance, fungi are capturing the middle phase of research on the biological production of metallic nanoparticles.[17] Ellagic acid, piliformic acid, cytochalasin D, phenolic derivatives, polyphenols, dihydroxybenzene, presence of OH groups, and many aromatic ring

compounds extracted from fungal biomass are used to synthesize metallic nanoparticles such as zinc, copper, gold, silver, iron, and some other metal oxide nanoparticles.[18–20] The ZnO substrate is surrounded by secondary metabolites present in the fungal extract and becomes stable by polymerization, leading to the formation of nanostructures of ZnO NPs.[21] Another benefit of using fungi in production is the simplicity in their scale-up. Since fungi are extremely proficient secretors of extracellular enzymes, rapid large-scale production of enzymes is possible.[22] Additional, favorable features of utilizing a fungal-mediated natural method for the production of metallic nanoparticles include simplicity in handling biomass and economic viability.[23] Along with preferences for using natural methods, endeavors are increasing to achieve nanoparticle production utilizing fungal secondary metabolites over physical and chemical production methods.[24]

The extensive use of already available drugs has led to the evolution of multi-drug resistant organisms (MDROs), meaning medicines that were previously highly active are now limited in their efficacy. A primary concern is to tackle infections involving multi-drug resistant bacteria.[25] ZnO NPs can generate Zn^{2+} ions, which can fix to a bacterial surface and form reactive oxygen species (ROS), resulting in an undesirable condition surrounding the bacteria. ZnO NPs possess antimicrobial activity against many pathogenic organisms such as bacteria and fungi by penetrating the bacterial cell wall and cell membrane. Such divergent behaviors of ZnO NPs make them effective for use as antibacterial agents against pathogenic microbes such as Gram-positive and Gram-negative bacteria.[26]

The second most common cause of cancer death in women is breast cancer.[27] Due to the rapid development of resistance to already available chemotherapeutic agents and to minimize their side effects, biological methods to enhance cancer treatment are needed.[28] Metallic nanoparticles can accomplish the targeted delivery of drugs to cancer cells. Some important inorganic nanoparticles such as zinc oxide, silver, gold, iron oxide, gadolinium, and titanium dioxide are used in cancer treatment. Out of all of these, ZnO nanorods (ZnO NRs) are exceptional with their wide applications in imaging, biosensing, cancer treatment, and gene delivery.[29–31]

In the present research, we described the extracellular synthesis of ZnO NPs through the extract of endophytic fungus, isolated from leaves of *Millingtonia hortensis* L.f. An attempt was made to find the antimicrobial activity of ZnO NPs. The anticancerous potential of the produced ZnO NPs was also examined.

Materials and Methods

Collection of Plant Materials and Isolation of Endophytic Fungi

The *Millingtonia hortensis* L.f. was collected and deposited. The plant authentication certificate was obtained from the Regional Ayurveda Research Institute for Metabolic Disorders, RARIMD, Bangalore. *Millingtonia hortensis* L.f. leaves were collected from the Bisle region of Western Ghats (Bisle region 10°10′N, 77°04′E). The plant's leaf samples were cleaned methodically with distilled water, blot dried, and rinsed in 70% ethanol (v/v) for 1 min, followed by rinsing with sodium hypochlorite (2.5%, v/v) solution for 2 min. The leaf samples were soaked three times with germ-free distilled water and desiccated on sterilized blotting sheets inside the laminar airflow to confirm the complete absence of moisture. Tissue segments of 5×5 mm size were cut out with the support of a sterilized blade. Five segments were plated per Petri plate with potato dextrose agar (PDA) medium procured from Hi-media. The Petri plates were covered with parafilm and kept for incubation at 28°C with 12 h light and dark cycles for 3–4 weeks. Periodically, the tissue segments were inspected for the fungal colony's appearance. Each colony that appeared from sections was shifted to antibiotic-free potato dextrose agar medium (PDA) to aid identification.[32,33]

Identification of Endophytic Fungi by the Morphological Method

The endophytic fungal cultures were first identified to morphospecies. The identified endophytic cultures were inoculated on different media depending on their ability to sporulate. Fungi growing out of the explants were identified in their sporulation state by staining with lactophenol cotton blue. Endophytic fungal isolates were identified based on morphological characteristics with the help of standard mycological manuals.[34] The following characters were used for the characterization and identification of morphospecies: mycelium color, colony appearance and structure, type of anamorph, conidia, and conidiophore morphology, and conidiogenous cells.[35]

Fungal DNA Isolation and Its Molecular Characterization

The obtained fungal isolate was grown in liquid culture medium utilizing 100 mL of potato dextrose broth medium (PDB) (Hi-Media, pH 7.2) in 250-mL conical flasks to acquire new fungal hyphal growth for DNA extraction. The centrifugation process at 10,000 rpm at 4°C for 8 min was carried out to separate mycelia. Liquid nitrogen was used for crushing the obtained mycelia. The fungal DNA was extracted from 100 mg of fungal mycelia suitable for the process.[36] PCR products were observed by gel electrophoresis technique with 2% (w/v) agarose gel. The amplification of the internal transcribed spacer (ITS) regions, which are universal primers of the fungal rRNA operon, were used to carry out the molecular characterization of fungi[37] (Sakhala enterprises, Research services, Bangalore, Karnataka).

### Preparation of Fungal Extract for ZnO NPs Synthesis

The *Xylaria acuta* was cultured in a 500 mL conical flask comprising 300 mL PDB at 26°C for 3 days on a shaker incubator. After the incubation period, the fungal biomass was separated from the PDB medium. The PDB medium without fungal mycelia of *Xylaria acuta* was centrifuged at 10,000 rpm for 15 min and followed by filtration through Whatman filter paper No. 1 and was stored in a sterile brown bottle at 4°C and used for further study.[38]

Synthesis of ZnO NPs

The precursor material zinc nitrate hexahydrate [$Zn(NO_3)_2.6H_2O$] was used for ZnO NPs synthesis. 1 g of $Zn(NO_3)_2.6H_2O$ was dissolved in 2–10 mL of fungal extract. This reaction mixture was stirred well with the help of a magnetic stirrer and kept in a pre-heated muffle furnace maintained at 400±10°C, and the final product was further calcinated at 700°C for 2 h.[39] Thus, synthesized ZnO NPs were also subjected to structural characterization (Figure 1). The ZnO NPs' size and structures are subject to nucleation and development energy from a supersaturated arrangement from these procedures, such as coarsening, focused connection, and accumulation.[40]

Characterization of ZnO NPs

Fabrication of nanoparticles was finalized through various spectroscopic and microscopic techniques. The ultraviolet-visible spectra of ZnO NPs was measured with optical densityusing a UV-Vis double beam spectrophotometer (Systronic Model Au2700) at 280–500 nm wavelength range.[41] The spectra of bio-inspired ZnO NPs of *Xylaria acuta* were examined in 2500 to 400 cm^{-1} range using an FTIR spectrophotometer (Varian 3100). The crystallinity of ZnO NPs was performed by a powder X-ray diffraction
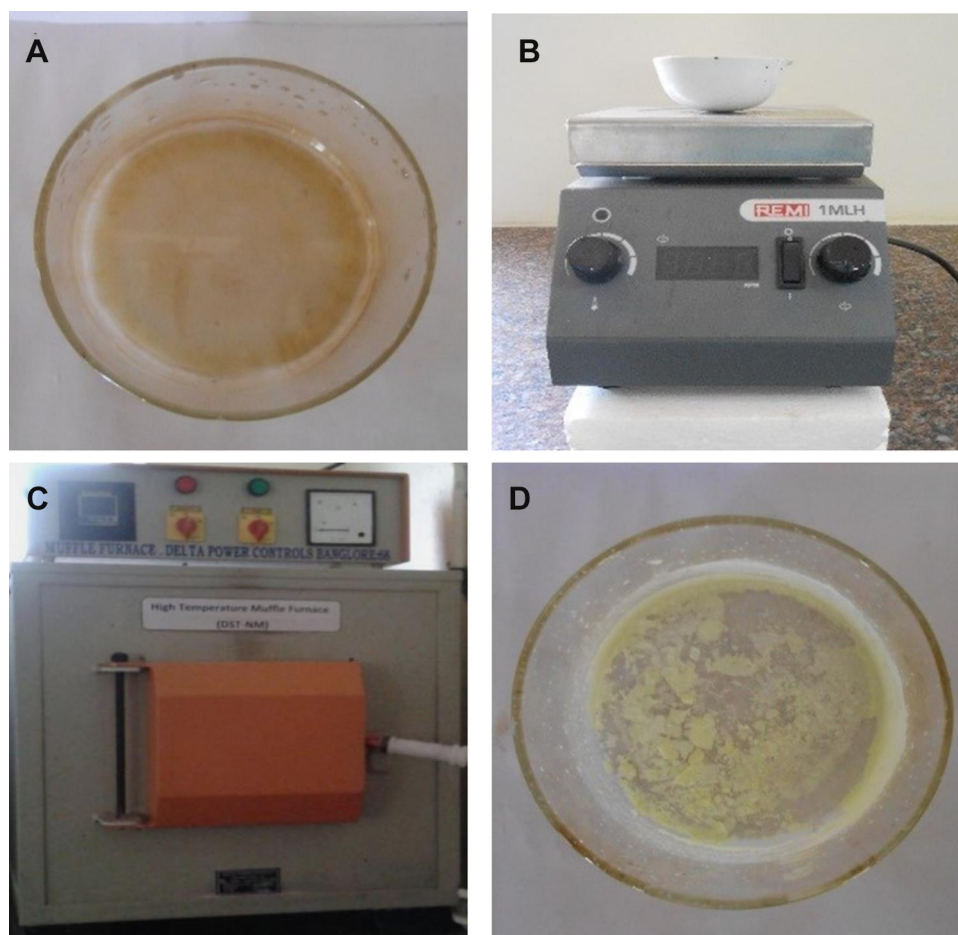
Figure 1 Synthesis of ZnO NPs from fungal extract. (**A**) zinc nitrate hexahydrate with fungal extract, (**B**) magnetic stirrer, (**C**) muffle furnace maintained at 400°C, and (**D**) final synthesized product.

(20–80°). An analytical X-ray diffractometer (Xrd, Shimadzu 7000), furnished with a Ni filtered utilizing Cu Kα (λ = 1.54056 Å) radiations as an X-ray source was used to obtain the PXRD pattern of ZnO nanopowder synthesized.[42] The synthesized ZnO NPs surface morphology was analyzed using scanning electron microscopy (SEM) (Vega3 Tescan-Jeol/Eo Jsm-5600). The elemental compositions of ZnO NPs were examined using energy-dispersive X-ray spectroscopy (EDX) (Jeol/Eo Jsm-5600 Sem analyzer).[43] The size distribution of the synthesized ZnO NPs was measured using dynamic light scattering (DLS) (Malvern, Zetasizer Ver. 7.11). DLS estimation, for the most part, depends on Rayleigh scattering from the suspended nanoparticles in the solution.[44] Transmission electron microscopy (TEM) together selective area electron diffraction (SAED) (Hitachi H7500) was used to determine the size of ZnO NPs.[45]

Bioactivity of ZnO NPs

Antibacterial Activity of ZnO NPs Synthesized from the Fungal Extract

The test organisms *Bacillus cereus* (NCIM No. 2016), *Staphylococcus aureus* (NCIM No. 2079), *Pseudomonas aeruginosa* (NCIM No. 2200), and *Escherichia coli* (NCIM No. 2556) were bought from the National Collection of Industrial Microorganisms (NCIM), Pune, India. Fungal crude extract (1mg/disc) and ZnO NPs (1 mg/disc and 0.5 mg/disc) was added to each sterile disc (Himedia SD067). Bauer and Kirby's method evaluated the antimicrobial activity on Muller Hilton agar (MHA) seeded with the 0.1 mL test bacterial suspension (10^6 cells) of each test organism. This was followed by incubation at 37°C for 24 h. 20 µL of DMSO was used as a negative control, and 20 µL of tetracycline (300 µg/mL) was used as a positive control.[46]

The broth microdilution procedure was utilized to determine the antibacterial potential of ZnO NPs by minimum inhibitory concentration (MIC) and minimum bactericidal concentration (MBC). The two-fold sequentially weakened stock of ZnO NPs was mixed with nutrient broth (NB) stock medium to get various concentrations (500 µg/mL to 7.80 µg/mL) and then added to each well of a clean 96-well microtiter plate. The 20 µL suspension of bacteria with 10^6 cells/mL concentration was added to each well and incubated for 24 h at 37°C.[47] A positive control of 30 µg/mL concentration of tetracycline was used. DMSO was considered as a blank control. After a 24 h incubation period, by adding 50 µL of iodonitrotetrazolium chloride (INT) (0.5 mg/mL) to all the wells, MIC values of the nanoparticles were determined, the trials were kept at 37°C for 1 h for incubation. The most minimal drug concentration that prevents colorless to red color alteration was determined as MIC. The colorless tetrazolium salt acting as an electron ++3 of refined stock (in the absence of INT) was streaked over the nutrient agar (NA) and kept for incubation at 37°C for 24 h, for assurance of MBC. The lowest concentration, which demonstrated the total absence of the growth of the bacteria on the agar surface, was considered as the MBC.[48]

Antifungal Activity

The antifungal potential of the produced ZnO NPs by fungal extract is estimated using plant pathogens (*Fusarium oxysporum, Phomopsis* sp.,) and common contaminants *Aspergillus flavus, Cladosporium cladosporioides* by the food-poison procedure with some alterations. The potato dextrose agar (PDA) autoclaved medium with ZnO NPs at the concentrations of 400, 300, 200, and 100 µg/mL were transferred into sterile Petri plates. A Petri plate with a solution without ZnO NPs was considered as control. A 7-day-old culture disc of test samples was punched aseptically using an aseptic cork borer of 0.5 cm diameter and positioned at the center of Petri plates. The plates were kept for incubation at 28 ± 2°C. The given formula calculated the inhibition of mycelia in percentage:[49]

$$\text{Percentage of mycelial inhibition} = \frac{\text{Mycelial growth}_{(control)} - \text{Mycelial growth}_{(treatment)}}{\text{Mycelial growth}_{(control)}}$$

Anticancer Activity

Human MDA-MB 134 mammary gland carcinoma cells were commercially purchased from the National Center for Cell Science (NCCS), Pune, Maharashtra, and cell line analysis was performed in the Department of Microbiology and Biotechnology, Bangalore University. The review committee of the Department of Microbiology and Biotechnology, Bangalore University, approved the use of the human MDA-MB 134 mammary gland carcinoma cell line in our experiments. The cells kept in Leibowitz's Medium (L-15 medium) were used with minor modifications for qualitative apoptosis and cell uptake study. The human MDA-MB 134 mammary gland carcinoma cells were seeded in 6-well plates (Costars, Corning Inc., NY, USA) at the density of 5×10^4 cells per well. Additionally, to confirm the viability of the human MDA-MB 134 mammary gland cancer cell line a MTT assay was performed by seeding 1×10^4 cells per well in 96-well cell culture plates (Costars, Corning Inc., NY, USA).[50]

Cell Uptake Profile by Confocal Microscopy

The human MDA-MB 134 mammary gland carcinoma cells were incubated with samples (fungal extract/ZnO NPs) at 1 µg/mL concentration for 180 min. After the incubation period, the media containing samples (fungal extract/ZnO NPs) were extracted and examined under a confocal laser microscope (Olympus FV1000) after being washed three times with Hanks buffered salt (HBS) solution (PAA Laboratories GmbH, Austria).[30] Caspase-8, 9, and 3 assays were performed using the caspase assay kit; the procedure was carried out as described by the manufacturer. Human MDA-MB 134 mammary gland carcinoma cells were then loaded in 96-well plates and were seeded with 5×10^5 cells and treated with the samples (fungal extract and ZnO NPs) at a concentration of 1 µg/mL then allowed to incubate for 1 day at CO_2 atmosphere. Later, cancer cells were treated with appropriate caspases 8, 9, and 3 reagents and then kept in a darkroom for 2 h. Green fluorescence was detected at 530 nm when excited at 503 nm.[31]

MTT Assay

MTT assay was performed to evaluate the cell cytotoxicity of fungal extract and ZnO NPs samples in human MDA-MB 134 mammary gland carcinoma cells. In short, the cell lines were seeded in 96-well plates and kept for incubation along with L-15 media comprising samples of fungal extract and ZnO NPs cells. The cell lines treated with blank media were considered healthy blank, and the cells treated with Triton X-100 with a comparable concentration of 0.1 to 1µg/mL was regarded as the negative control.

After an incubation time of 1 day, the L-15 media consisted of aspirated samples, and cells were washed with HBS several times. Later, 150 µL of MTT solution (500 µg/mL in phosphate buffer solution) was complemented to all wells and kept for incubation again for 4 h. Subsequently, the mixture of formazan crystals was dissolved in 200 µL of DMSO once the MTT solution was carefully aspirated. Utilizing an ELISA plate reader (BioTek, USA), the subsequent solution's absorbance was measured at 570 nm.[51]

Apoptosis Assay

The apoptosis mechanism was evaluated, employing flow cytometry to confirm samples' anticancer potential (fungal extract/ZnO NPs). The phosphatidylserine (PS) translocation exposure, a governing factor of apoptosis mechanism in cell lines, was analyzed by employing annexin V-FITC/PI Vybrant apoptosis assay kit (Molecular Probes, Eugene, OR, USA). The process involved cell seeding in 8-well plates having a density of 1×10^4/well. The cells attaining 90% confluency were then treated with samples (fungal extract/ZnO NPs) and incubated for exposure for about 24 hours at 37°C. After incubation time, the cells were collected by trypsinization and eroded with PBS pH 7. They were centrifuged at 4000 rpm for 3 min at 5°C. The particles obtained on centrifugation were kept in ice-cold Annexin binding buffer. About 2 µL of annexin V-FITC solution and 1 µL of PS (100 µg/mL) were supplemented to 100 µL of the cell suspension system and mixed carefully. The test samples were kept for incubation for 20 min. The samples were mixed with 500 µL of the ice-cold 1X binding buffer after incubation. The samples were carefully mixed and scanned for flow cytometry (FACS Aria II, Beckton, and Dickinson, Sanjose, CA). The results were reported as the mean of triplicate measurements, along with standard deviation.[50,52,53]

Statistical Analysis

The mean ± SE results obtained were subjected to multivariate analysis. Means are separated by Tukey's multiple range test at 0.5 significance ($P < 0.05$) using graph pad prism software.

Results
Isolation and Molecular Identification of Endophytic Fungi

The collected plant was deposited in the Regional Ayurveda Research Institute for Metabolic Disorders, RARIMD, Bangalore. The plant was identified as *Millingtonia hortensis* L.f. and given a reference number (RRCBI-mus210) (Table 1). A total of 14 fungal endophytes were isolated from the leaves of *Millingtonia hortensis* L.f. The obtained endophytic fungal isolates can be seen in Figure 2. *Xylaria acuta* was one among the 14 endophytic fungi isolated and used to synthesize ZnO NPs, and was selected for further studies.

The genus *Xylaria* consists of grooved, club-like decomposers of timber or plant remains that become black and hard by maturity, with the appearance of carbon or charcoal. The fungi are "Ascomycetes," which means they generate spores in asci that are implanted in little pockets called "perithecia"; once the asci grows, they make a turn into the narrow opening of the pocket so that they can shoot spores into the airaway from the fungus (Figure 3A). The ascospores produced, which are oval, can be observed in Figure 3B. It has a fruiting body that is sturdy and shaped more or less like a club or finger, but sometimes flattened, as can be seen in Figure 3C. Conidia are with a circular tip, with an outer covered with pale blue, purplish residue or whitish tip.[33]

Xylaria acuta was the fungal isolate obtained, its presence was confirmed by molecular identification, and it was selected for further studies. The phylogenetic tree obtained after the molecular characterization is shown in Figure 3D.[34] The ITS1-5.8S-ITS2 gene complex sequences of isolated fungi were deposited into the GenBank database of NCBI and given accession number MH362730 (Table 2).

Characterization of ZnO NPs
UV-VIS Spectrometer Analysis

The UV spectrum, which showed a distinct peak at 370 nm, confirms the reduction of zinc ions to ZnO NPs. The fungus-synthesized nanoparticles appear to be white, suspended (1 mg/mL) in distilled water, and used for UV-Vis spectroscopic reading. Ultraviolet-visible spectra had a maximum absorption peak at 370 nm, which can be seen in Figure 4. The different volumes of fungal extract 2 mL, 4mL, 6 mL, 8 mL, and 10 mL showed peaks at 370.24, 370.73, 370.02, 370.24, and 370.09 nm, respectively. The obtained absorption peaks that represent ZnO NPs were in good agreement with the earlier studies in which absorption peaks were from 355–380 nm.[39]

Fourier Transform Infrared (FT-IR) Spectroscopy

The FT-IR spectrum of fungus-promoted ZnO shows the phenolic OH groups present in the IR spectrum and

Table 1 Medicinal Plant Selected for Endophytic Fungal Isolation and Their Reference Number After Deposition in RARIMD, Bangalore

Sl. No.	Plant Sample	Geographical Location	Isolation Period	Reference Number
I	*Millingtonia hortensis* L.f.	Bisle region 10° 10'N, 77°04'E	Dec 2018	RRCBI-mus210

confirms the possible mechanism for the formation of ZnO NPs utilizing fungal extract, as can be observed in Figure 5. The ZnO formation involves the hydroxyl groups, and polyphenols were depicted from the obtained IR spectrum. Also, the peaks observed due to the aromatic ring system in the range 1466–1472 cm^{-1} might be allotted to the C=C stretch. The fragile bands depicted keto-enol in the field of 10,341–1034 cm^{-1}, and 517–524 cm^{-1} could be because of CAH stretch (alkanes) and CAH stretch (aromatics) functional groups. The CAC stretching of aromatic rings in the synthesis of ZnO was seen in absorption peaks ranging from 1100–1105 cm^{-1}.[43] The spectrum revealed an increased peak in transmittance was observed at 386.07 cm^{-1}, 385.11 cm^{-1}, 401.40 cm^{-1}, 389.90 cm^{-1} and 389.90 cm^{-1} to 2, 4, 6, 8, and 10 mL respectively and accredited to a vibrational metal-oxide band. The peak in the range of 380 cm^{-1} to 580 cm^{-1} was assigned to metal oxide.[54]

Figure 2 Isolation of endophytic fungi from *Millingtonia hortensis* L.f. leaves.

Powder X-Ray Diffraction

The biosynthesized ZnO nanostructure using the fungal extract of *Xylaria acuta* was verified and finalized by the PXRD graph's distinctive peaks. The PXRD graphs of ZnO NPs synthesized from different fungal extract concentrations (2 mL to 10 mL) are shown in Figure 6. The PXRD peaks obtained belong to the plane 100, 002, 101, 102, 110, 200, 103, 112 and 201 with the 2θ values of 31.36, 34.21, 36.13, 47.39, 56.49, 62.81, 66.23, 68.05, and 69.16 respectively. There were no characteristic peaks from other phases or impurities; hence the product obtained is of pure phase ZnO NPs. The diffraction peaks confirm the presence of pure ZnO in the hexagonal wurtzite structure.[43] Comparison with the data from JCPDS card No. 89–7102, with the obtained PXRD results, confirms the ZnO with no other characteristic peaks. The average size of the obtained ZnO NPs was calculated using Scherrer's formula applied to the first intense PXRD peaks. The average calculated diameter of the particle was about 35–45 nm (Table 3). The synthesized nanoparticles are in the nanometer range as confirmed by line broadening of the diffraction peaks.[45]

$$D = \frac{0.9 \mathrm{x} \lambda}{\beta \cos \theta}$$

Whereλ is used wavelength, i.e., X-ray (1.542 Å), β is full width at half maximum (FWHM in radian) caused by the crystallites, θ is the Bragg angle. Table 3 summarizes the estimated values of ZnO NPs size for the prepared samples.

Scanning Electron Microscopy

Several nanoparticle combinations and the distinct ZnO NPs were witnessed in the SEM micrographs (Figure 7A–D). The ZnO nanoparticle structures were cylindrical rod and hexagonal shape. When observed under magnification of 500 nm, various hexagonal nanoparticles were noticeably evident. The SEM images exhibited the creation of combinations of nanoparticle crystals; at a better magnification of 500nm straight molecules with hexagonal-like shape were observed in Figure 7E. As depicted using the SEM images, the hexagonal nanoparticle diameter was 40–55 nm on average. The EDX was processed to decide the elemental composition and presence of the ZnO NPs. EDX spectrum depicted a strong signal for zinc and oxygen. The result of EDX confirmed the ZnO NPs by fungal-mediated synthesis, the existence of the element zinc in its oxide form rather than in pure zinc form (Figure 7A–E).[48]
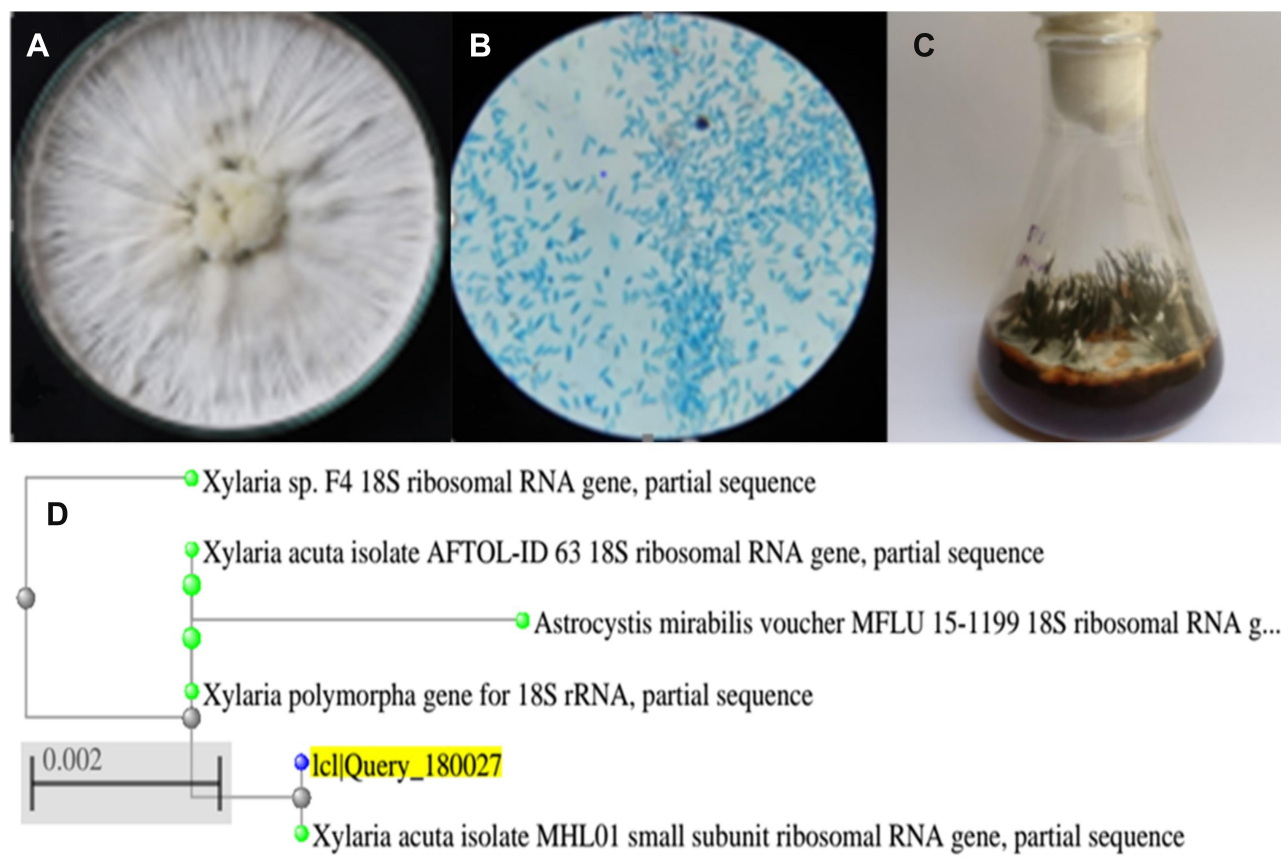
Figure 3 (**A**) Pure culture of *Xylaria acuta*. (**B**) Microscopic view of *X. acuta* (40×), (**C**) Fruiting body *X. acuta*, and (**D**) Phylogenetic tree of *X. acuta*.

Among the synthesized ZnO NPs from the fungal extracts (2 mL to 10 mL), ZnO NPs synthesized from 10 mL of fungal extracts show better antimicrobial activity against bacteria and fungi than synthesized ZnO NPs from the other volumes of fungal extracts. Hence DLS and TEM with SAED were conducted for ZnO NPs synthesized from the 10 mL of fungal extract sample to confirm the size of the ZnO NPs.

Dynamic Light Scattering Analysis of ZnO NPs

The DLS technique revealed the particle size of synthesized ZnO NPs (10 mL) using the fungal extract from

Table 2 Molecular Characterization of Isolated Fungi and Accession Number Obtained After Submission of the Database to NCBI

Sl. No.	Fungi	Isolation Source	Isolation Period	Accession Number
I	*Xylaria acuta*	Leaves	Dec 2018	MH362730

distributed ZnO NPs suspension. The DLS size distribution image of bio-fabricated ZnO NPs is shown in Figure 8A. The ZnO NPs size distribution was observed in the range of ~20 to ~105nm (Figure 8B) with the maximum size distribution of around 30–50 nm (Figure 8B) and an average size of 52 nm (Figure 8A). The DLS analyzer showed a broad spectrum that confirms that the nanoparticle size decreases when matched with the sharp peak (370 nm) found in the ultraviolet-visible spectrum.[44]

Transmission Electron Microscopy

The TEM micrographs of ZnO NPs synthesized from fungal extract (10 mL) are shown in Figure 9A. The TEM results depict the well-dispersed minute particles of agglomerated ZnO NPs, which are hexagonal. The TEM analysis also revealed that the particle size of ZnO NPs synthesized ranges from 30 to 50 nm. The PXRD profile's prominent peaks were in good agreement with the corresponding values of SAED patterns (Figure 9B).[45] The average size of the synthesized ZnO NPs using *X. acuta* fungal extract (10 mL) was ~34 nm. A substantial amount
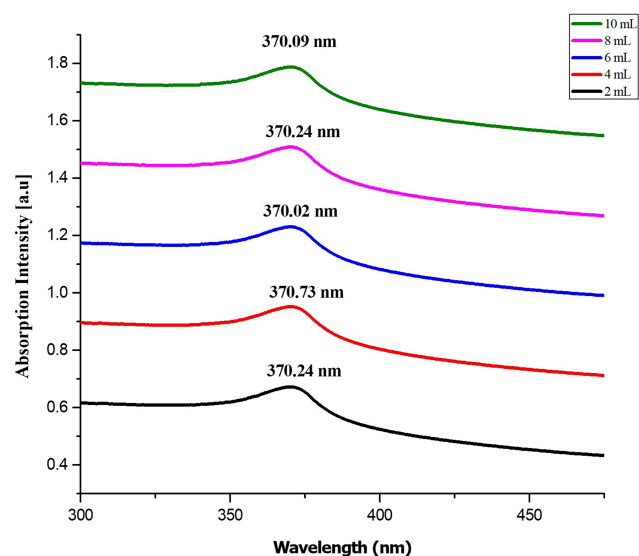
Figure 4 UV-visible absorbance spectra of ZnO NPs synthesized from different volumes of fungal extract (2 to 10 mL).

of mostly hexagonal ZnO NPs within the range of 50 nm was observed in TEM micrographs (Figure 9A).[55]

Antibacterial Activity

The antibacterial activity assessed by disc diffusion method and crude fungal extract depicted that 1 mg concentration of synthesized ZnO NPs showed an inhibition zone. In contrast, the crude fungal extract did not show significant inhibition (Table 4). Hence, ZnO NPs were further studied for the determination of MBC and MIC against test bacteria. The antibacterial properties of ZnO

NPs in contrast to human pathogens were assessed, using a broth microplate dilution method (Gram-positive and Gram-negative bacteria).[18] Different concentrations of ZnO NPs were added exponentially to cultured bacteria and incubated for 1 day. Bacteria cultured in the absence of ZnO NPs functioned as a control. Table 5 shows the MIC and MBC values of all fungal synthesized ZnO NPs (2–10 mL) trials compared with bacteria.[44] Different concentrations of ZnO NPs exhibited prominent inhibition against *B. cereus, S. aureus, E. coli*, and *P. aeruginosa* with notable changes in the susceptibility to ZnO NPs. The fungal-synthesized ZnO NPs showed antimicrobial activity in a dosage reliant method, i.e., the concentration of the ZnO NPs increased, so did the antimicrobial activity.[41] Among the test bacteria, *S. aureus* and *B. cereus* are depicted as highly susceptible to ZnO NPs with MIC concentration 15.6 μg/mL, followed by *E. coli* and *P. aeruginosa* with MIC concentration of 31.3 μg/mL (Table 5).[46]

In contrast, *E. coli* was shown to be minimally effective. The composition of the Gram-positive and Gram-negative cell wall plays a significant role in the antibacterial mechanism.[45] The antibacterial activity of ZnO NPs towards the test bacteria depends on the specific surface area, morphology, powder concentration, particle size, etc.[47] The H_2O_2 (highly reactive species) that is responsible for the penetration of bacterial cell wall might be another reason for better antibacterial activity.[48] Thus abrasive action on the cell wall is caused by the smaller sized, efficient nanoparticles. It might be the reason for membrane
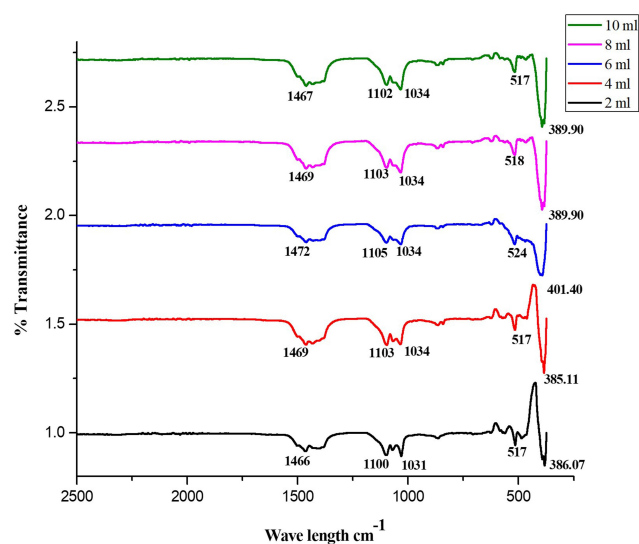
Figure 5 FTIR spectra transmittance of ZnO NPs synthesized from different volumes of fungal extract (2 to 10 mL).
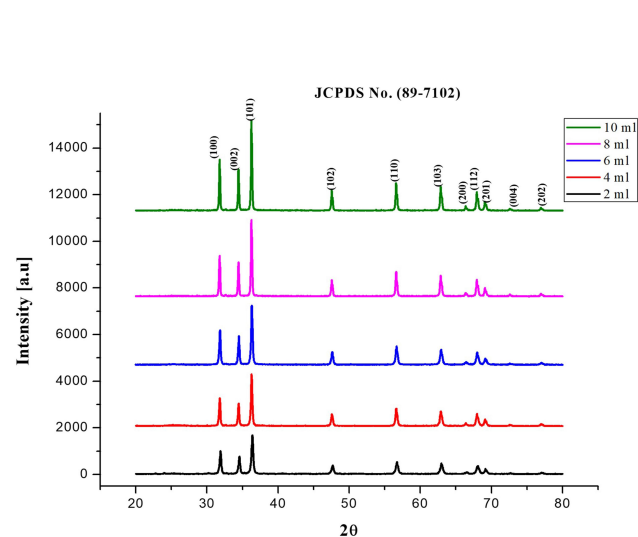
Figure 6 PXRD peaks of synthesized ZnO NPs using different volumes of fungal extract (2 to 10 mL).

Table 3 The Estimated Values of ZnO NPs Size for Different Volumes of Fungal Extract Using Scherrer's Formula

The Concentration of Fungal Extract Used for ZnO NPs Synthesis	Scherrer's Formula D (nm)
2 mL	44
4 mL	41
6 mL	39
8 mL	36
10 mL	34

damage. Hence, the stable ZnO NPs synthesis would be suitable for knowing the antibacterial potential (Table 5).[56]

Antifungal Activity

The ZnO NPs acquired with a concentration of 10 mL were used for antifungal activity. ZnO NPS antifungal effect at different concentrations (100, 200, 300, and 400 μg/mL) was tested against plant pathogenic and common contaminating fungi (*Aspergillus flavus, Phomopsis* sp., *Fusarium oxysporum, Cladosporium cladosporioides*) were verified using the food-poison method.[16] The results revealed different concentrations that depict mycelia's predicted inhibition in a dose-dependent way compared with all the fungi. *Fusarium oxysporum* is less vulnerable to ZnO NPs paralleled to *Aspergillus flavus* and *Phomopsis* sp. estimated in this study.[42] ZnO NPs synthesized were effective in inhibition of mycelia of *Cladosporium cladosporioides* (Table 6). Based on the obtained results, ZnO NPs are in good agreement that they can control fungi, plant pathogenic and common contaminants effectively. The ZnO NPs synthesized interact with fungal membrane sterols physicochemically and help in the fungistatic mechanism by mycelial inhibition.[54] Also, it is beneficial to lead an exact mechanism of restraint investigations of the fungi.

Anticancerous Activity

Ten milliliters of fungal extract-synthesized ZnO NPs showed significant antimicrobial activity against bacteria and fungi. Hence further anticancerous activity was conducted for ZnO NPs synthesized from 10 mL of fungal extract and crude fungal extract.

Cell Uptake Analysis

The cell uptake analysis of ZnO NPs illustrated by confocal laser scanning microscopy suggests that a significant amount of ZnO NPs (1 μg/mL) was internalized and distributed without the disturbance of morphological and structural

human MDA-MB 134 mammary gland carcinoma cells compared with fungal extract of *Xylaria acuta* (1 μg/mL) (Figure 10A and B; a, b, c and d) at 6 and 12 hours.[13,14] There are two underlying mechanisms for ZnO NPs internalization: the first endocytosis and the second cell-binding mechanisms. This cell surface binding helps in substantial uptake and conveyance, leading to the remarkable endocytosis phenomenon.[18] Briefly, synthesized ZnO NPs exhibited capable and significant cell uptake and internalization due to the nanosize range of nanoparticles compared with fungal extract, size reliant endocytosis, and cell surface binding subsequent in proficient antibacterial and anticancerous activity in vitro.[30] Figure 10A and B; g and h depict the cell uptake by demonstrating the superimposition of figures showing vertical and horizontal line series analysis of the figure's fluorescence along the white line of fungal extract and ZnO NPs.

Caspase-8, 9, are the enzymes responsible for the initiation of apoptosis. Caspase-3 effector caspases function to cleave protein substrates and carry forward apoptosis. Then, the suitable caspase-3 reagents including four amino acid peptides comprise the recognition site for caspases 3 conjugated to nucleic acid binding dye, and these were allowed to treat the cancer cells.[30] Since the DEVD peptide constrains the dye's capacity to fix DNA, the green detection reagent is nonfluorescent. In the existence of initiated caspase-3, the dye is sliced from the DEVD peptide and permitted to fix DNA. It generates a light green fluorescent signal as revealing apoptosis (Figure 10A and B; e and f).[31]

MTT Assay

The MTT assay exhibited that synthesized ZnO NPs are cytocompatible and naturally safe at all the concentrations when utilized against human MDA-MB 134 mammary gland carcinoma cells. The human MDA-MB 134 mammary gland carcinoma cells were found sustainable at varying concentrations viz., 0.1,1, 5, 10, and 20 μg/mL when associated with negative control.[51] The cytotoxicity results indicated that synthesized ZnO NPs showed a decrease in toxicity towards the human MDA-MB 134 mammary gland carcinoma cell lines compared with the fungal extract of *Xylaria acuta*. The MTT cell viability due to pure ZnO NPs contact was decreased to 100%, 89%, 64%, 39%, and 21%. A fungal extract of *Xylaria acuta* exhibited 100%, 85%, 60%, 37%, and 18% at the concentrations of 0.1, 1, 5, 10, and 20 μg/mL, respectively; when *t*-test was performed, it was found statistically noteworthy (Figure 11). Furthermore, it matched with the negative
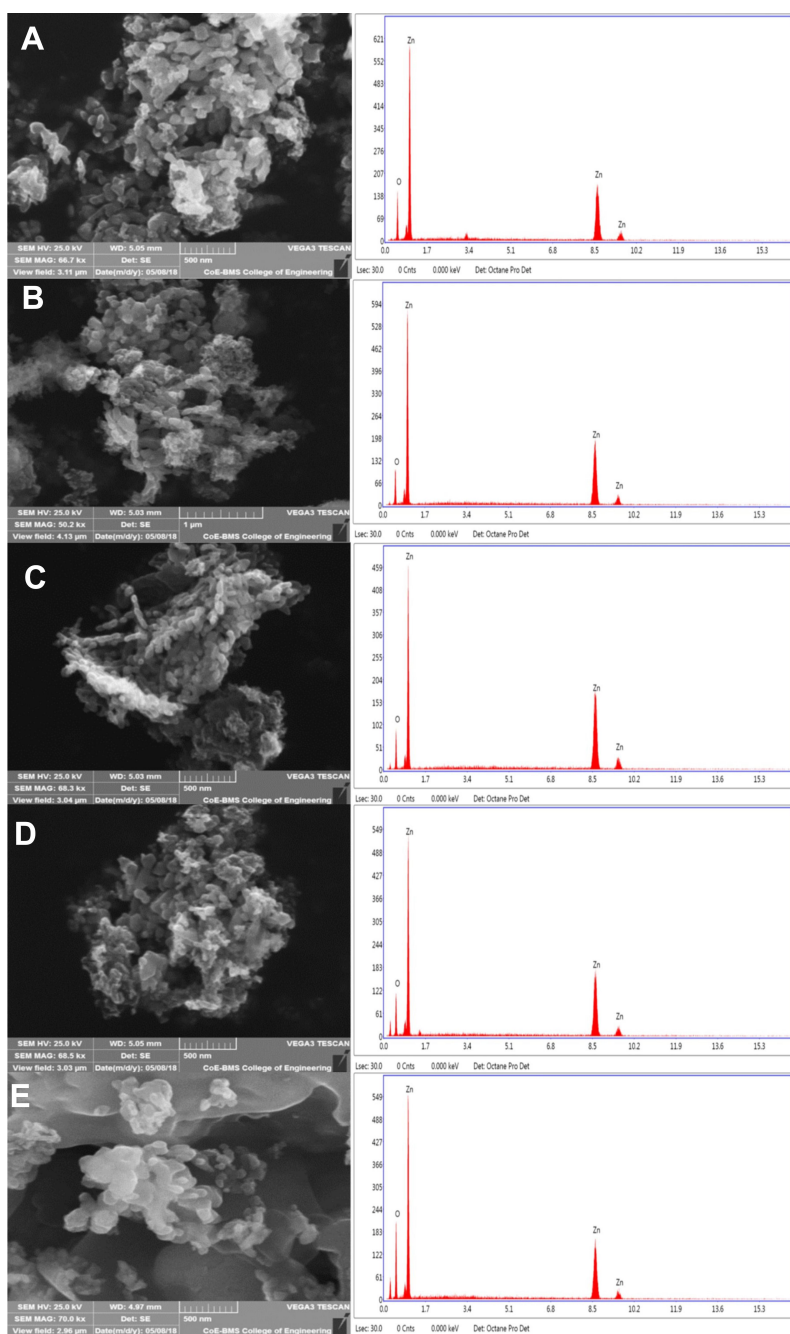
Figure 7 SEM micrographs with EDX graphs of ZnO NPs synthesized by different concentrations of fungal extract (**A**) 2 mL, (**B**) 4 mL, (**C**) 6 mL, (**D**) 8 mL, and (**E**) 10 mL of *Xylaria acuta* extract.

control. The IC$_{50}$ estimated by MTT assay was 6.589 for synthesized ZnO nanoparticles and 3.997 for *Xylaria acuta* fungal extract.[50,52]

Apoptosis Assay

The apoptosis assay employed on human MDA-MB 134 mammary gland carcinoma cell lines revealed remarkable apoptosis at the higher concentrations for longer incubation time when estimated by flow cytometer.[53] At different incubation intervals, the apoptosis shown by fungal extract of *Xylaria acuta* (red curve) and ZnO NPs (blue curve) when equated with Triton X (green curve) as standard is shown in Figure 12. The flow cytometer results recommended that synthesized ZnO NPs exhibited improved apoptosis and cell death at higher concentrations when incubated for a longer duration (12 h).[56]
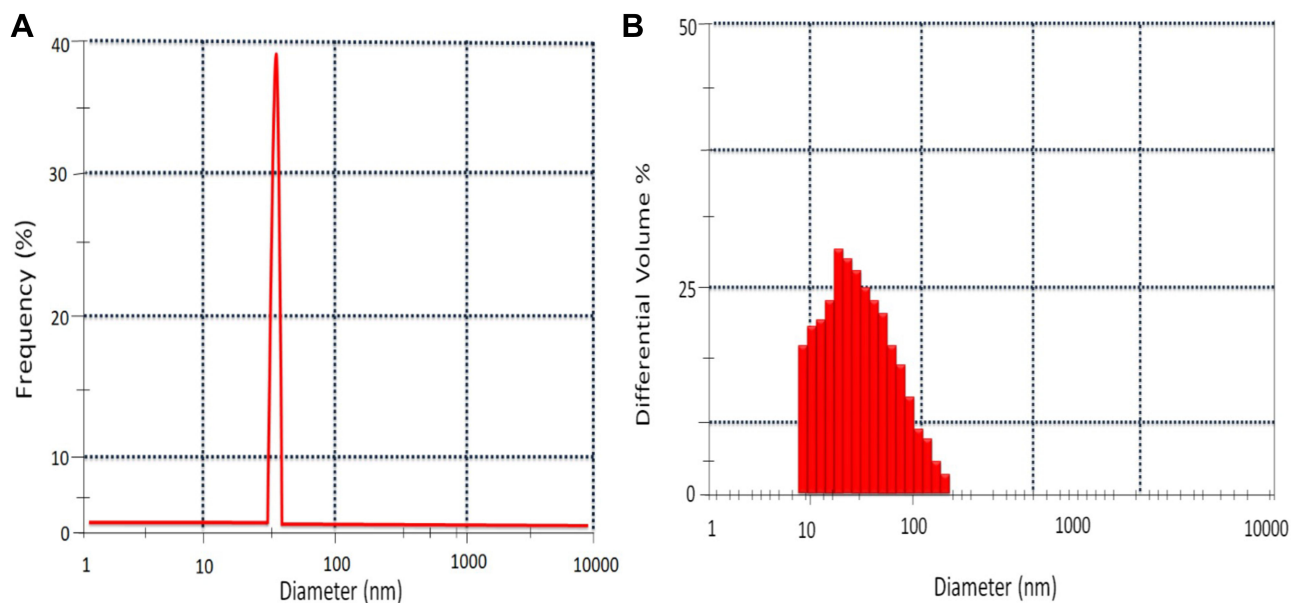
Figure 8 DLS of ZnO NPs prepared using 10mL of fungal extract (**A**) DLS peak showing the average size at 52nm. (**B**) ZnO NPs showing distribution in the range of 30 nm to 50 nm.

Discussion

Nanotechnology is a powerful, empowering technology in applied science that deals with the control of substances on a molecular scale.[1] The physical and chemical methods of synthesizing nanoparticles have their disadvantages because of radiation and involvement of toxic chemicals.[2] The biological synthesis of nanoparticles is a low-cost, high yielding, non-toxic, and environmentally benign approach with high interest.[3] A wide range of biological resources existing in nature, both unicellular and multi-cellular organisms such as bacteria, viruses, algae, yeast, fungi, actinomycetes, plants, and plant products are known to produce inorganic materials.[4] These inorganic materials can be intracellular or extracellular and could be employed in the synthesis of metallic nanoparticles.[7] Fungi are the center of interest in studies of biological synthesis of metallic nanoparticles due to their metal accumulation ability and tolerance to metals.[24] The synthesis of the
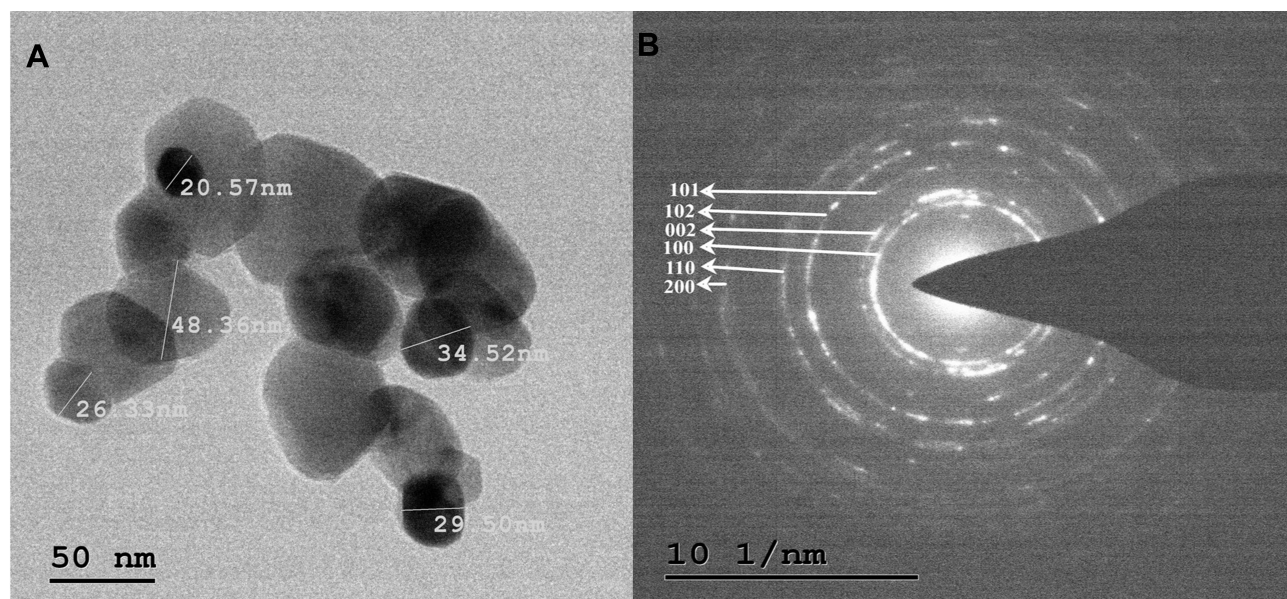
Figure 9 TEM micrographs (**A**) and SAED patterns (**B**) of ZnO NPs synthesized by 10mL fungal extract of *X. acuta*.

Table 4 The Antibacterial Activity of ZnO NPs by Well Diffusion Method Was Carried Out Against Gram-Positive *Bacillus cereus* and *Staphylococcus aureus*, Gram-Negative *Pseudomonas aeruginosa*, and *Escherichia coli*

Drug Samples	Zone of Inhibition in mm			
	B. cereus	*S. aureus*	*P. aeruginosa*	*E. coli*
Positive control	7	6	7	5
Negative control	0	0	0	0
Fungal extract	1	0	1	0
ZnO NPs (0.5 mg/mL)	3	1	2	2
ZnO NPs (1 mg/mL)	3	2	3	3

ZnO NPs includes the cationic connections with the polymer network of the fungal extract of *Xylaria acuta*. The production of nanostructures can connect the networks among reducing secondary metabolites present in the fungal extract. The possible cause for variation in the size and structure of ZnO NPs is the rise in the concentration of secondary metabolites of *Xylaria acuta* extract. The contents such as surfactants and reductants manage ZnO's nucleation mechanism, necessary in the ZnO nanostructures' organized growth.[54] Yuvakkumar et al. did a similar

Table 5 The Antibacterial Activity (MIC and MBC) Was Carried Out Against Gram-Positive *Bacillus cereus*, and *Staphylococcus aureus*, Gram-Negative *Pseudomonas aeruginosa*, and *Escherichia coli* Expressed as μg/mL

The Concentration of Fungal Extract Used for ZnO NPs Synthesis		*B. cereus*	*S. aureus*	*P. aeruginosa*	*E. coli*
2 mL	MIC	62.5	125	250	125
	MBC	125	250	500	500
4 mL	MIC	62.5	125	125	125
	MBC	125	250	500	250
6 mL	MIC	31.3	62.5	62.5	62.5
	MBC	125	250	250	250
8 mL	MIC	31.3	31.3	62.5	31.3
	MBC	125	250	125	250
10 mL	MIC	15.6	15.6	31.3	31.3
	MBC	62.5	62.5	125	125

study using the Rambutan fruit peel where the phenolic OH^- groups of polyphenols and ester group of oxygen atom customize the p-track conjugation influence. The OH- groups formed by the chelating effect, combined with the metal as a metal phenolate complex (zinc-ellagate complex).[55] The ZnO NPs are synthesized when these complexes go through direct decomposition at $450^{\circ}C$.

The ultraviolet-visible spectrum distinguishing a prominent peak at 370 nm can be attributed to ZnO NPs.[54] The XRD peaks obtained in the current study are similar to the reported XRD patterns obtained for ZnO nanoparticles, which are synthesized using *Nerium oleander* leaf extract. The results were identical to that of the crystallographic hexagonal wurtzite structure of synthesized nanoparticles. The hexagonal structure was achieved by a one-step green synthesis of ZnO NPs using *Nerium oleander* leaf extract as a precursor (zinc nitrate hexahydrate).[39] The SEM analysis showed the cylindrical rods and hexagonal structures of ZnO NPs, which resembles the nanoparticle produced by Mohamed et al. The energy dispersive spectroscopy of *Xylaria acuta* extract was analogous to the data described in other studies.[38] In another study of ZnO NPs from leaf extract, the size range of the biologically produced nanoparticles was similar to the range of nanoparticles synthesized by our work.[47,48] The fungal-synthesized ZnO NPs are competent antibacterial representatives, as reported previously.[18] The bio-fabricated ZnO NPs from fungal sources influenced antibacterial mechanisms compared with food-borne pathogens such as *S. aureus, E. coli, S. typhimurium, B. subtilis*, and *P. fluorescens*.[41,46] The study carried out by Lakshmeesha et al. suggests that the size and shape of the ZnO NPs influence the antimicrobial activity where ZnO NPs synthesized showed noticeable results of both MIC and MBC effectively against the tested bacteria.[39] The leading cause of bacterial inhibition is the formation of reactive oxygen species (ROS), where H_2O_2 molecules can penetrate the bacterium cell wall. The reason behind the increased antimicrobial activity in a dose-dependent manner is the increasing concentration of H_2O_2 at the surface of ZnO. Hence, ZnO NPs shows better antimicrobial activity, when compared with other metal oxide nanoparticles such as FeO, CdO, and Ag NPs.[48]

Comparable outcomes have also been reported. Studies found that ZnO NPs prevent the development of *Proteus morganii, E. coli*, and *Klebsiella* sp.[47,49] The results obtained from the antifungal activity of ZnO NPs synthesized by fungal extract is in good agreement with a similar study carried out on *Rhizopus oryzae*. A similar antifungal

Table 6 Antifungal Activity of ZnO NPs from the Fungal Extract by Food-Poison Method Was Carried Out for *A. flavus, Phomopsis* sp., *F. oxysporum*, and *C. cladosporioides*

| Organisms	PC (1µg/mL)	400 µg/mL	300 µg/mL	200 µg/mL	100 µg/mL	NC
A. flavus	100	74.16±0.095[a]	54.16±0.170[b]	30.83±0.170[c]	12.22±0.216[d]	0
Phomopsis sp.	100	63.05±.095[a]	40.55±.057[b]	26.7±.057[c]	13.61±.095[d]	0
F. oxysporum	100	59.72±.0957[a]	41.94±.189[b]	29.16±.05[c]	18.88±.081[d]	0
C. cladosporioides	100	92.77±.057[a]	75.27±.09[b]	66.66±.081[c]	30.27±.095[d]	0

Notes: The above detailed values signify the diameter of the disc. Interpretations are stated as mean ± standard error (n = 3). The different alphabets (a - most significant, b - more significant, c - moderately significant, and d- significant compared to the control) followed by the readings diverge significantly when subjected to Turkey HSD (row by row analysis) P-value ≤0.05.

survey was carried out by Saqib et al. for different fungal pathogens.[6,49] Miri et al. assessed the antifungal activity of ZnO NPs against *Candida albicans*, and ZnO NPs showed better antifungal activity against *Candida*.[11] The study of targeted delivery of various drugs towards cancer cells and repairing them with the help of nanoparticles is one of the exciting applications of nanotechnology in the field of medicinal chemistry.[14,28] Synthesized ZnO NPs showed
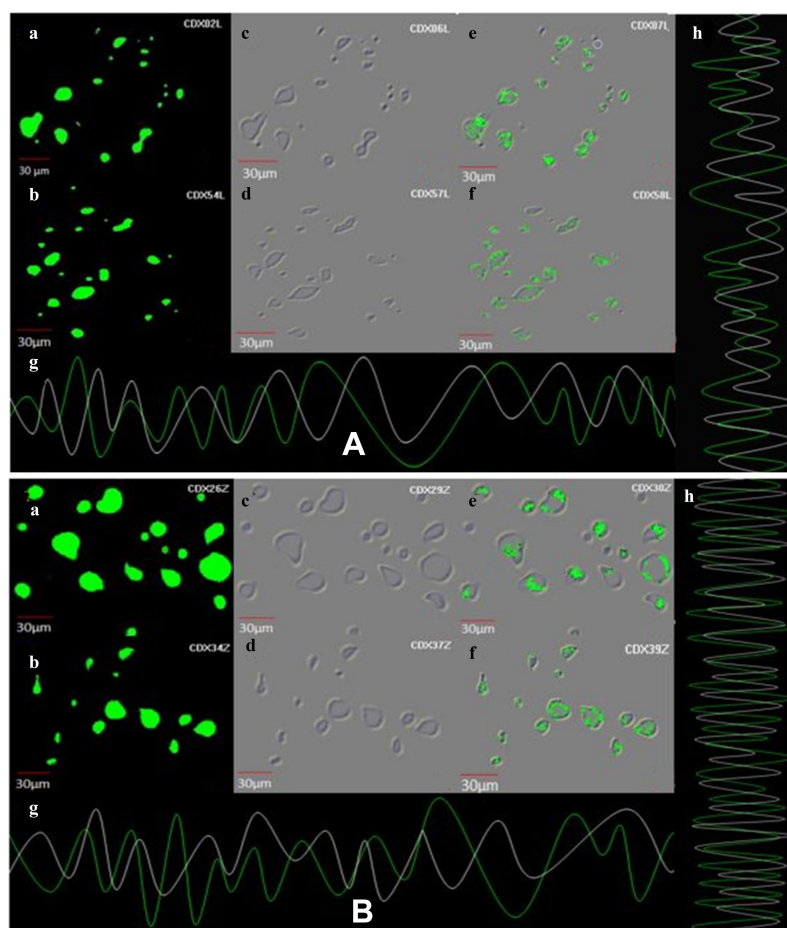

Figure 10 (**A**) Demonstration of cell uptake assay by CLSM, images at 6 h and 12 h (a and b) showing cell uptake of fungal extract, images (c and d) exhibiting cell uptake by fungal extract on human MDA-MB 134 mammary gland carcinoma cell lines exhibiting under the green fluorescence channel along with differential interface contrast images at 6 h and 12 h, image (e and f) shows the caspase-3 reagents along with fungal extract binding to the nuclei of cancer cell lines images at 6 h and 12 h. (g and h) demonstrating superimposition of figures showing vertical and horizontal line series analysis of fluorescence of figure along the white line. (**B**) Demonstration of cell uptake assay by CLSM at 6 h and 12 h, images (a and b) showing cell uptake of ZnO NPs, images (c and d) exhibiting cell uptake by ZnO NPs on human MDA-MB 134 mammary gland carcinoma cell lines exhibiting under the green fluorescence channel along with differential interface contrast images at 6 h and 12 h (e and f) shows the caspase-3 reagents along with ZnO NPs binding to the nuclei of cancer cell lines image at 6 h and 12 h. (g and h) demonstrating superimposition of figures showing vertical and horizontal line series analysis of fluorescence of figure along the white line.

MTT Assay of ZnO NPs Against MDA MB-134
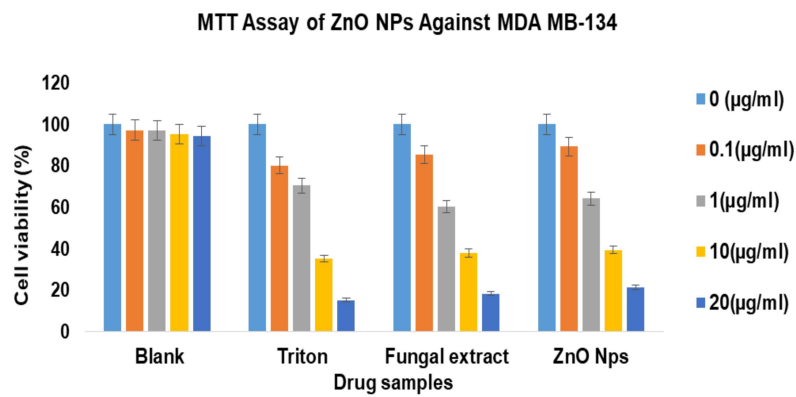
Figure 11 MTT assay on human MDA-MB 134 mammary gland carcinoma cell lines against zinc oxide nanoparticles and fungal extract along with triton as control at different concentration on 24 h of incubation.

prominent results in cell line studies by cell uptake mechanism, caspase-3 activity, MTT assay, and apoptosis assay, which were in line with the studies of Sahu.[50,51] A study by Gurunathan on MDA-MB-231 breast cancer cell line indicated the potential cytotoxic effect of biologically synthesized Ag NPs was similar to our study where the
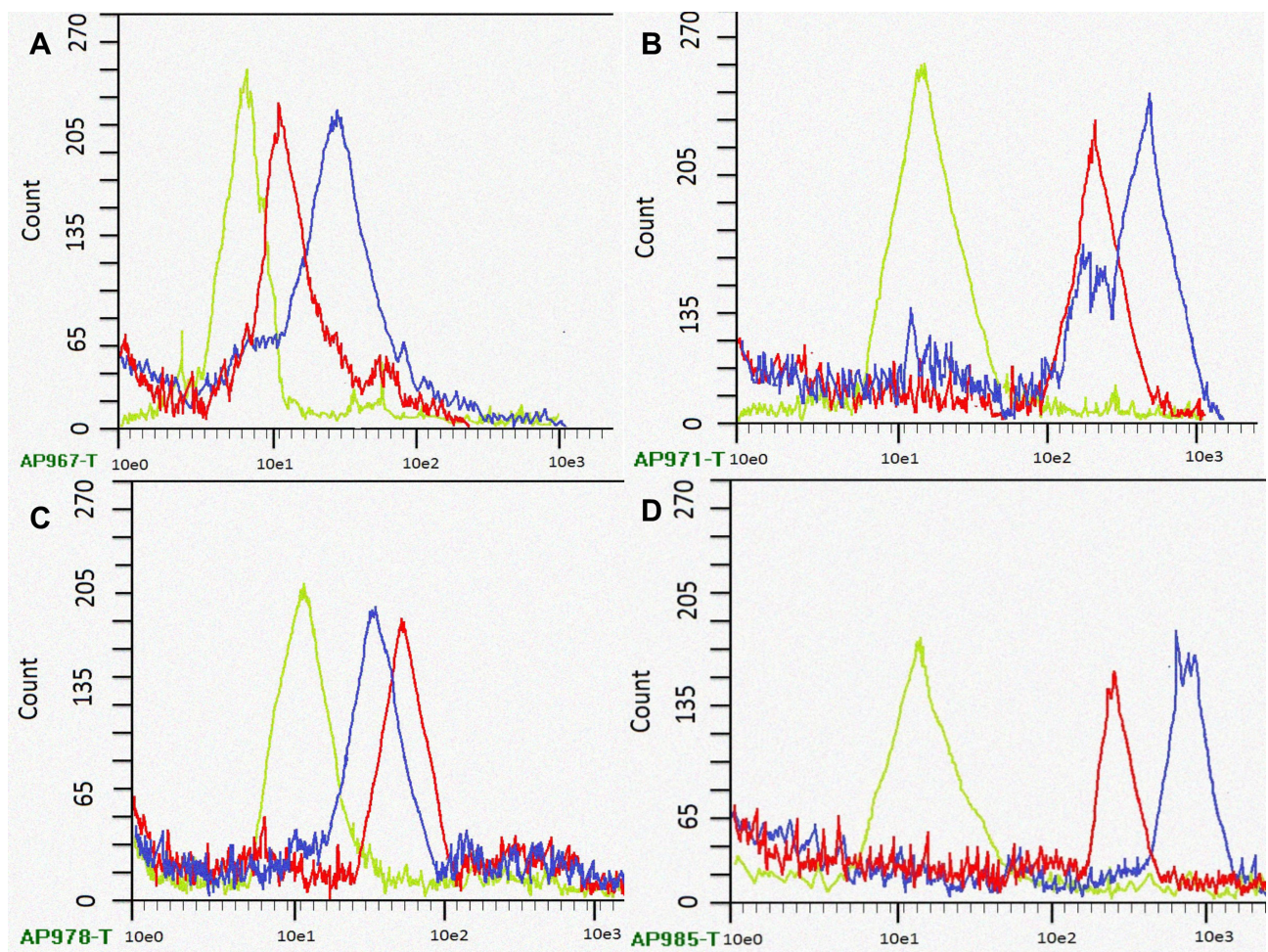
Figure 12 Flow cytometric graphs showing apoptosis cell populations measured by flow cytometry at different time intervals of human MDA-MB 134 mammary gland carcinoma cell lines cultured with standard Triton X (green channel curve), fungal extract (red channel curve) and synthesized ZnO NPs using fungal extract (blue channel curve) respectively, ((**A**) 2 h, (**B**) 4 h, (**C**) 8 h, and (**D**) 12 h of incubation).

growth of the cancer cells was inhibited by increasing the ROS generation and activation of caspase-3.[57] Caspases cause cellular apoptosis, the reason behind this is oxidative stress being involved in ZnO NPs cytotoxicity.[6] The Khatua et al. study reveals the importance of ZnO in the release of ROS in control of human colon cancer cells, which enhances the use of ZnO NPs in cancer treatment.[30] Similar research by Kim focuses on the importance of ZnO NPs in targeted drug delivery for treating cancer cells.[14,28] There is a drawback to using toxic chemicals, and the process consumes more time during the synthesis of metallic nanoparticles.[58] These metallic nanoparticles also harm human health if consumed as drugs. Hence, biologically mediated synthesis of ZnO NPs is preferred with a lower concentration of zinc.[4,49]

Conclusion

The current study highlights the fungal-mediated synthesis of ZnO NPs utilizing fungal extract of *Xylaria acuta*. The characterization of produced nanopowder was done using ultraviolet-visible spectroscopy, FT-IR, PXRD, SEM with EDX, DLS, and TEM with SEAD to expose the synthesis of ZnO nanoparticles. This study focuses on fungi-mediated synthesis of ZnO NPs using a simple and eco-friendly method, which is novel, harmless, and cost-effective compared with physical and chemical synthesis. The particles have better morphologies and have a nanosize efficient for inhibition of microbes. ZnO NPs synthesized through fungal-mediated synthesis have predominant microbicidal effects against pathogens. Here, from our results, we emphasize that the synthesized ZnO NPs can be used as potent antimicrobial agents. Further, the anticancer activity results indicated that the fungal-mediated synthesized ZnO NPs have antiproliferative activity against human MDA-MB 134 mammary gland carcinoma cells, suggesting they can be potential anticancer agents.

Acknowledgment

Disclosure

References

1. Happy A, Venkat KS, Rajesh KS. A review on green synthesis of zinc oxide nanoparticles eco-friendly approach. *Resour Effic Technol*. 2017;3:406–413. doi:10.1016/j.reffit.2017.03.002
2. Barabadi H, Tajani B, Moradi M, et al. Penicillium family as an emerging nano factory for the biosynthesis of green nanomaterials: a journey into the world of microorganisms. *J Clust Sci*. 2019;1–14.
3. Narayanan KB, Han SS. Icosahedral plant viral nanoparticles - bioinspired synthesis of nanomaterials/nanostructures. *Adv Colloid Interface Sci*. 2017;248:1–19. doi:10.1016/j.cis.2017.08.005
4. Kaushik NT, Snehit SM, Rasesh YP. Biological synthesis of metallic nanoparticles. *Nanomed Nanotechnol*. 2010;6:257–262. doi:10.1016/j.nano.2009.07.002
5. Shen T, Wang Q, Liu C, Yu F, Yu D, Li C. *Euphorbia milii* extract-mediated zinc oxide nanoparticles and their antinociceptive, muscle relaxant, and sedative activities for pain management in pediatric children. *Appl Nanosci*. 2020;10:1297–1303. doi:10.1007/s13204-019-01210-2
6. Shobha N, Nanda N, Giresha S, et al. Synthesis and characterization of zinc oxide nanoparticles utilizing seed source of *Ricinus communis* and studying its antioxidant, antifungal, and anticancer activity. *Mat Sci Eng C*. 2019;97:842–850. doi:10.1016/j.msec.2018.12.023
7. Ahmed S, Chaudhry SA, Ikram S, Ikram S. A review on biogenic synthesis of ZnO nanoparticles using plant extracts and microbes: a prospect towards green chemistry. *J Photochem Photobiol B*. 2017;166:272–284. doi:10.1016/j.jphotobiol.2016.12.011
8. AmithYadav HJ, Eraiah B, Nagabhushana H, et al. Bio-inspired ultrasonochemical synthesis of blooming flower-like ZnO hierarchical architectures and their excellent biostatic performance. *J Sci Adv Mat*. 2017;2(4):455–469.
9. Singh RP, Shukla VK, Yadav RS, Sharma PK, Singh PK, Pandey AC. The biological approach of zinc oxide nanoparticles formation and its characterization. *Adv Mater Lett*. 2011;2(4):313–317. doi:10.5185/amlett.indias.204
10. Xu J, Chen Z, Zapien JA, Lee CS, Zhang W. Surface engineering of ZnO nanostructures for semiconductor-sensitized solar cells. *Adv Mater*. 2014;26(31):5337–5367.
11. Miri A, Khatami M, Ebrahimy O, Sarani M. Cytotoxic and antifungal studies of biosynthesized zinc oxide nanoparticles using the extract of *Prosopis farcta* fruit. *Green Chem Lett Rev*. 2020;13(1):27–33. doi:10.1080/17518253.2020.1717005
12. Ali K, Dwivedi S, Azam A, et al. *Aloe vera* extract functionalized zinc oxide nanoparticles as nanoantibiotics against multi-drug resistant clinical bacterial isolates. *J Colloid Interface Sci*. 2016;472(2):145–156. doi:10.1016/j.jcis.2016.03.021
13. Barabadi H, Ovais M, Shinwari ZK, Saravanan M. Anti-cancer green bionanomaterials: present status and prospects. *Green Chem Lett Rev*. 2017;10(4):285–314. doi:10.1080/17518253.2017.1385856
14. Zhihong Y, Ye Y, Pejhan A, Nasr AH, Nourbakhsh N, Tayebee R. A theoretical study on the pure and doped ZnO nanoclusters as effective nano biosensors for 5-fluorouracil anticancer drug adsorption. *Appl Organomet Chem*. 2020;34(4):e5534. doi:10.1002/aoc.5534
15. Zheng Y, Fu L, Han F, et al. Green biosynthesis and characterization of zinc oxide nanoparticles using *Corymbia citriodora* leaf extract and their photocatalytic activity. *Green Chem Lett Rev*. 2015;8(2):59–63. doi:10.1080/17518253.2015.1075069
16. He L, Liu Y, Mustapha A, Lin M. Antifungal activity of zinc oxide nanoparticles against *Botrytis cinerea* and *Penicillium expansum*. *Microbiol Res*. 2011;166(3):207–215. doi:10.1016/j.micres.2010.03.003
17. Barabadi H, Honorary S, Mohammadi MA, et al. Green chemical synthesis of gold nanoparticles by using *Penicillium aculeatum* and their scolicidal activity against hydatid cyst protoscolices of *Echinococcus granulosus*. *Environ Sci Pollut Res*. 2017;24(6):5800–5810.

18. Zhang L, Jiang Y, Ding Y, Povey M, York D. The investigation into the antibacterial behavior of suspensions of ZnO nanoparticles (ZnO nanofluids). *J Nanopart Res*. 2007;9:479–489. doi:10.1007/s11051-006-9150-1

19. Shih YH, Chang KW, Hsia SM, et al. In vitro antimicrobial and anticancer potential of hinokitiol against oral pathogens and oral cancer cell lines. *Microbiol Res*. 2013;168(5):254–262. doi:10.1016/j.micres.2012.12.007

20. Barabadi H, Honary S, Ebrahimi P, Alizadeh A, Naghibi F, Saravanan M. Optimization of myco-synthesized silver nanoparticles by response surface methodology employing Box-Behnken design. *Inorg Nano Met Hem*. 2019;49(2):33–43. doi:10.1080/24701556.2019.1583251

21. Kalpana VN, Kataru BAS, Sravani N, Vigneshwari T, Panneerselvam A, Rajeswari VD. Biosynthesis of zinc oxide nanoparticles using culture filtrates of *Aspergillus niger*: antimicrobial textiles and dye degradation studies. *Open Nano*. 2018;3:48–55.

22. Raliya R, Tarafdar JC, Biswas P. Enhancing the mobilization of native phosphorus in the mung bean rhizosphere using ZnO nanoparticles synthesized by soil fungi. *J Agric Food Chem*. 2016;64 (16):3111–3118. doi:10.1021/acs.jafc.5b05224

23. Tarafdar JC, Agrawal A, Raliya R, Kumar P, Burman U, Kaul RK. ZnO nanoparticles induced synthesis of polysaccharides and phosphatases by *Aspergillus fungi*. *Adv Sci Eng Med*. 2012;4(4):324–328. doi:10.1166/asem.2012.1160

24. Ganesan V, Hariram M, Vivekanandhan S, Muthuramkumar S. *Periconium sp.* (endophytic fungi) extract mediated sol-gel synthesis of ZnO nanoparticles for antimicrobial and antioxidant applications. *Mater Sci Semicond Process*. 2020;105:104739. doi:10.1016/j.mssp.2019.104739

25. Rajivgandhi G, Maruthupandy M, Muneeswaran T, Anand M, Manoharan N. Antibiofilm activity of zinc oxide nanosheets (ZnO NSs) using *Nocardiopsis sp*. GRG1 (KT235640) against MDR strains of gram-negative *Proteus mirabilis* and *Escherichia coli*. *Process Biochem*. 2018;67:8–18. doi:10.1016/j.procbio.2018.01.015

26. Ramachandrappa LT, Kalagatur NK, Mohan CD, et al. Biofabrication of zinc oxide nanoparticles with *Syzygium aromaticum* flower buds extract and finding its novel application controlling the growth and mycotoxins of *Fusarium graminearum*. *Front Microbiol*. 2019;10:1244. doi:10.3389/fmicb.2019.01244

27. Du XL, Fox EE, Lai D. Competing causes death for women with breast cancer and changes over time from 1975 to 2003. *Am J Clin Oncol*. 2008;31(2):105. doi:10.1097/COC.0b013e318142c865

28. Kim JH, Yoo HI, Kang HS, Ro J, Yoon S. Salinomycin sensitizes antimitotic drugs-treated cancer cells by increasing apoptosis via the prevention of G2 arrest. *Biochem Biophys Res Commun*. 2012;418 (1):98–103. doi:10.1016/j.bbrc.2011.12.141

29. Vahidi H, Barabadi H, Saravanan M. Emerging selenium nanoparticles to combat cancer: a systematic review. *J Clust Sci*. 2020;31 (2):301–309. doi:10.1007/s10876-019-01671-z

30. Khatua A, Prasad A, Priyadarshini E, et al. Emerging antineoplastic plant-based gold nanoparticle synthesis: a mechanistic exploration of their anticancer activity toward cervical cancer cells. *J Clust Sci*. 2019;1–12.

31. Zhao C, Zhang X, Zheng Y. Biosynthesis of polyphenols functionalized ZnO nanoparticles: characterization and their effect on the human pancreatic cancer cell line. *J Photochem Photobiol B*. 2019;183:142–146. doi:10.1016/j.jphotobiol.2018.04.031

32. Fazilath U, Srinivas C. Antimicrobial and antioxidant potential of endophytic fungi isolated from ethnomedicinal plants of Western Ghats, Karnataka. *J Pure Appl Microbiol*. 2017;11(2):1009–1025. doi:10.22207/JPAM.11.2.43

33. Pradeepa VS, Vittal RR. Diversity and bioactive potential of endophytic fungi from *Nothapodytes foetida, Hypericum mysorense*, and *Hypericum japonicum* collected from Western Ghats of India. *Ann Microbiol*. 2015;66(1):321–335.

34. Ellis MB, Ellis JP. *Microfungi on Land Plants: An Identification Handbook*. London: Croom Helm Ltd; 1985.

35. Gilman JC. *A Manual of Soil Fungi*. Calcutta: Oxford and IBH publishing company; 1959.

36. Romina G, Priscila C. Diversity of fungal endophytes in leaves and stems of wild rubber trees (*Hevea brasiliensis*) in Peru. *Fungal Ecol*. 2010;3(3):240–254. doi:10.1016/j.funeco.2009.12.001

37. Ramesha A, Sunitha VH, Srinivas C. Antimicrobial activity of secondary metabolites from endophytic fungi isolated from *Nerium oleander* L. *Int J Pharm Bio Sci*. 2013;4(1):683–693.

38. Mohamed AA, Fouda A, Abdel-Rahman MA, et al. Fungal strain impacts the shape, bioactivity, and multifunctional properties of green synthesized zinc oxide nanoparticles. *Biocatal Agric Biotechnol*. 2019;19:101103. doi:10.1016/j.bcab.2019.101103

39. Lakshmeesha TR, Sateesh MK, Daruka PK, et al. Reactivity of crystalline ZnO superstructures against fungi and bacterial pathogens: synthesized using leaf extract. *Cryst Growth Des*. 2014;14(8):4068–4079. doi:10.1021/cg500699z

40. Hussain I, Singh NB, Singh A, Singh H, Singh SC. Green synthesis of nanoparticles and its potential application. *Biotechnol Lett*. 2016;38(4):545–560. doi:10.1007/s10529-015-2026-7

41. Yuvakkumar R, Suresh J, Joseph NA, Sundararajan M, Hong SI. Novel green synthetic strategy to prepare ZnO nanocrystals using rambutan (*Nephelium lappaceum* L.) Peel extract and its antibacterial applications. *Mater Sci Eng C*. 2014;41:17–27. doi:10.1016/j.msec.2014.04.025

42. Pragati J, Poonam K, Rana JS. Green synthesis of zinc oxide nanoparticles using flower extract of *Nyctanthes arborists* and their 42al activity. *J King Saud Univ Sci*. 2018;30:168–175. doi:10.1016/j.jksus.2016.10.002

43. Anand A, Nussana L, Sham Aan MP, Ekwipoo K, Sangashetty SG, Jobish J. Synthesis and characterization of ZnO nanoparticles and their natural rubber composites. *J Macromol Sci B*. 2020;1–16.

44. Ahn MW, Park KS, Heo JH, et al. Gas sensing properties of defect-controlled ZnO-nanowire gas sensor. *Appl Phys Lett*. 2008;93 (26):263103. doi:10.1063/1.3046726

45. Lepot N, Van Bael MK, Van den Rul H, et al. Synthesis of ZnO nanorods from aqueous solution. *Mater Lett*. 2007;61(13):2624–2627. doi:10.1016/j.matlet.2006.10.025

46. Mutlu EC, Yıldırım AB, Yıldırım M, et al. Improvement of antibacterial and biocompatibility properties of electrospray biopolymer films by ZnO and MCM-41. *Polym Bull*. 2019;1–19.

47. Da Silva BL, Caetano BL, Chiari-Andréo BG, Pietro RCLR, Chiavacci LA. Increased antibacterial activity of ZnO nanoparticles: influence of size and surface modification. *Colloid Surf B*. 2019;177:440–447. doi:10.1016/j.colsurfb.2019.02.013

48. Shankar S, Rhim J-W. Effect of Zn salts and hydrolyzing agents on the morphology and antibacterial activity of zinc oxide nanoparticles. *Environ Chem Lett*. 2019;17(2):1105–1109. doi:10.1007/s10311-018-00835-z

49. Saqib S, Zaman W, Ullah F, Majeed I, Ayaz A, Hussain Munis MF. Organometallic assembling of chitosan-Iron oxide nanoparticles with their antifungal evaluation against *Rhizopus oryzae*. *Appl Organomet Chem*. 2020;33(11):e5190.

50. Sahu P, Kashaw SK, Kushwah V, Sau S, Jain S, Iyer AK. pH-responsive 5- fluorouracil loaded biocompatible nanogels for topical chemotherapy of aggressive melanoma. *Colloids Surf B Biointerfaces*. 2019;174:232–245.

51. Ko CH, Shen SC, Hsu CS, Chen YC. Mitochondrial-dependent, reactive oxygen species-independent apoptosis by myricetin: roles of protein kinase C, cytochrome c, and caspase cascade. *Biochem Pharmacol*. 2005;69:913–927. doi:10.1016/j.bcp.2004.12.005

52. Maqusood A, Javed AK, Majeed K, Ahmad A. Zinc oxide nanoparticles selectively induce apoptosis in human cancer cells through reactive oxygen species. *Int J Nanomedicine*. 2012;7:845–857.

53. Kanagamani K, Muthukrishnan P, Shankar K, Kathiresan A, Barabadi H, Saravanan M. Antimicrobial, cytotoxicity and photocatalytic degradation of norfloxacin using *Kleinia grandiflora* mediated silver nanoparticles. *J Clust Sci*. 2019;30(6):1415–1424. doi:10.1007/s10876-019-01583-y

54. Healy PC, Hocking A, Tran-Dinh N, et al. Xanthones from a micro fungus of the genus *Xylaria*. *Phytochem*. 2004;65(16):2373–2378. doi:10.1016/j.phytochem.2004.07.019

55. Yuvakkumar R, Suresh J, Saravanakumar B, Joseph NA, Sun IH, Rajendran V. Rambutan peels promoted biomimetic synthesis of bioinspired zinc oxide nano chains for biomedical applications. *Spectrochim Acta A*. 2015;137:250–258. doi:10.1016/j.saa.2014.08.022

56. Lingaraju K, Naika HR, Nagabhushana H, Nagaraju G. *Euphorbia heterophylla* (L.) mediated fabrication of ZnO NPs: characterization and evaluation of antibacterial and anticancer properties. *Biocatal Agric Biotechnol*. 2019;18:100894. doi:10.1016/j.bcab.2018.10.011

57. Gurunathan S, Han JW, Eppakayala V, Jeyaraj M, Kim JH. Cytotoxicity of biologically synthesized silver nanoparticles in MDA-MB-231 human breast cancer cells. *Biomed Res Int*. 2013;535–544.

58. Mortezaee K, Najafi M, Samadian H, Barabadi H, Azarnezhad A, Ahmadi A. Redox interactions and genotoxicity of metal-based nanoparticles: a comprehensive review. *Chem Biol Interact*. 2019;312:108814. doi:10.1016/j.cbi.2019.108814